Received 28 August 2018; revised 2 October 2018; accepted 7 October 2018. Date of publication 12 October 2018; date of current version 1 March 2019. The review of this paper was arranged by Editor A. G. U. Perera.

Digital Object Identifier 10.1109/JEDS.2018.2875755

Electrical Stability of Solution-Processed a-IGZO TFTs Exposed to High-Humidity Ambient for Long Periods

SEUNG-UN LEE AND JAEWOOK JEONG

School of Information and Communication Engineering, Chungbuk National University, Cheongju 362-763, South Korea

CORRESPONDING AUTHOR: J. JEONG (e-mail: jjeong@cbnu.ac.kr)

This work was supported in part by the National Research Foundation of Korea funded by the Korean Government under Grant NRF-2017R1D1A1B03035271, and in part by the Ministry of Science and ICT, South Korea, through the Information Technology Research Center support program supervised by the Institute for Information & Communications Technology Promotion under Grant IITP-2018-2015-0-00448.

ABSTRACT The variations in the electrical and mechanical properties of solution-processed amorphous indium–gallium–zinc–oxide thin-film transistors exposed to high-humidity ambient conditions for long periods were analyzed. When the TFT was exposed to high-humidity conditions, field-effect mobility severely decreased, while ON/OFF current ratio improved and subthreshold slope value remained nearly constant, which is different from that exposed to low-humidity condition. We found that the H_2O molecules induce mechanical peeling of the active layer such that they act as acceptor-like deep states, which is very different from the prior results under low humidity condition. The variations in electrical characteristics were systematically analyzed using a technology-CAD simulation before and after exposure to high-humidity conditions.

INDEX TERMS a-IGZO, thin film transistor, humidity, stability, ambient.

I. INTRODUCTION

Solution-processed amorphous indium–gallium–zinc–oxide thin-film transistors (a-IGZO TFTs) have been widely studied to replace conventional vacuum-based TFTs for applications in various display and flexible electronic circuits [1]–[4]. One of the important issues for the a-IGZO TFTs is environmental stability under O_2 and H_2O ambient [5]–[7]. There have been significant efforts to investigate the role of various ambient for oxide-based TFTs [8], [9]. In particular, it has been understood that O_2 and H_2O act as acceptor [10] and donor-like [11], [12] states in a-IGZO TFTs, respectively. However, compared to vacuum-deposited a-IGZO TFTs, solution-processed TFTs are much more sensitive to the environment because more coarse packing of the active layer molecules leads to an increase in the absorption of various environmental gases [13], similar to the case for pore-structured thin films. In particular, exposure of the active layer to H_2O critically affects the electrical and mechanical properties of a-IGZO TFTs. It is necessary to investigate the effect of the long-period exposure to ambient water on the active layer, because the stability also critically depends on the exposure time of the ambient. In addition, the ambient effect should be studied for a very long time over several years under moderate-humidity conditions, which is the typical TFT operation condition in practical applications [14]. However, it is impossible to perform the humidity stability experiments such a long time in a research level. Instead, to study such an effect in a relatively short time, a harsh condition such as high humidity is typically used after removing a passivation layer. Accordingly, it is possible to predict the effect of water vapor to the active layer when exposed to very long time only using short time measurement results. In addition, the underlying physics of the active layer of solution-processed a-IGZO TFTs exposed to high humidity for very long periods has hitherto not been clearly investigated together with the mechanical and electrical characteristics.

In this study, we investigate the high-humidity exposure effect on the solution-processed a-IGZO TFTs for up to six days. To study the variation in mechanical properties,

2168-6734 © 2018 IEEE. Translations and content mining are permitted for academic research only.
Personal use is also permitted, but republication/redistribution requires IEEE permission.
See http://www.ieee.org/publications_standards/publications/rights/index.html for more information.

atomic force microscopy (AFM) nano-indentation was used to analyze the hardness variations for different humidity conditions. We accurately analyzed the effect of the low and high humidity conditions on solution-processed a-IGZO TFT considering density of state variation and surface morphology variations. We found a mechanical peeling of the active layer by water absorption, which induces an increase in acceptor-like traps, leading to a compensation of oxygen vacancies and a decrease in the field-effect mobility for long-period high-humidity conditions.

II. EXPERIMENT

The a-IGZO active layer solution was prepared using indium nitrate hydrate ($In(NO_3)_3xH_2O$), gallium nitrate hydrate ($Ga(NO_3)_3{\cdot}xH_2O$), and zinc acetate dehydrate ($Zn(C_4H_6O_4)2{\cdot}H_2O$) in 2-methoxyethanol ($C_3H_8O_2$). The molecular concentration of the solution was 0.05 M with In:Ga:Zn = 6:1:4. The molecular ratio was chosen as an optimum point from various conditions, which is similar with reported results in [15] and [16]. Arsenic doped silicon substrate (n + Si) was prepared, which also acts as a back gate electrode. The SiO_2/Si substrate was prepared using a dry oxidation process. The substrate was treated by oxygen plasma (power : 100 W, pressure : 1.4 torr) to improve adhesion property between the substrate and the a-IGZO active layer. After plasma treatment, the contact angle of de-ionized water was nearly zero indicating high adhesion property of the a-IGZO active layer. The solution was spin coated on the prepared substrate at a rotation speed of 4000 rpm. After spin coating, all samples were annealed using a muffle furnace at 400 °C for 2 hours in ambient helium. Then, 200 nm-thick Al source/drain (S/D) electrodes were deposited using a thermal evaporator at a deposition ratio of 2 Å/s. The fabrication of the TFT was performed in a glove box while maintaining the humidity under 20%. The channel length and channel width values were 1000 and 120 µm, respectively. Figure 1 shows a high-resolution transmission electron microscopy (HR-TEM; Model No. JEM-2100F) image of the a-IGZO TFT. The HR-TEM sample was prepared using focused ion beam milling technique (Model No. Helios NanoLab 450HP). The a-IGZO active layer thickness was about 8 nm and the active layer shows good adhesion to the SiO_2 gate insulator layer and Al electrode. After fabrication of the a-IGZO TFTs, initial measurements were performed (day 1). Then, the samples were divided into two pieces. One sample was stored in a chamber with a dry ambient of pure nitrogen with a relative humidity of under 5% (under 700 ppm, dry sample), and the other sample was stored in a wet ambient with a relative humidity of over 90% (over 13,000 ppm, wet sample) at room temperature. The variations in electrical characteristics were traced for six days. Before the TFT measurements, the variations of sheet resistance in the Al S/D electrodes were monitored. The sheet resistances were remained nearly the same values of 202.7 to 205.2 mΩ/square for different dry and wet conditions shown in Table 1. Accordingly, it is reasonable to assume that

TABLE 1. Resistance variations of Al electrodes depending on ambient conditions.

Time \ Ambient	Dry sample (mΩ/square)	Wet sample (mΩ/square)
1st day	205.2±8.9	
6th day	202.7±6.6	202.8±5.7

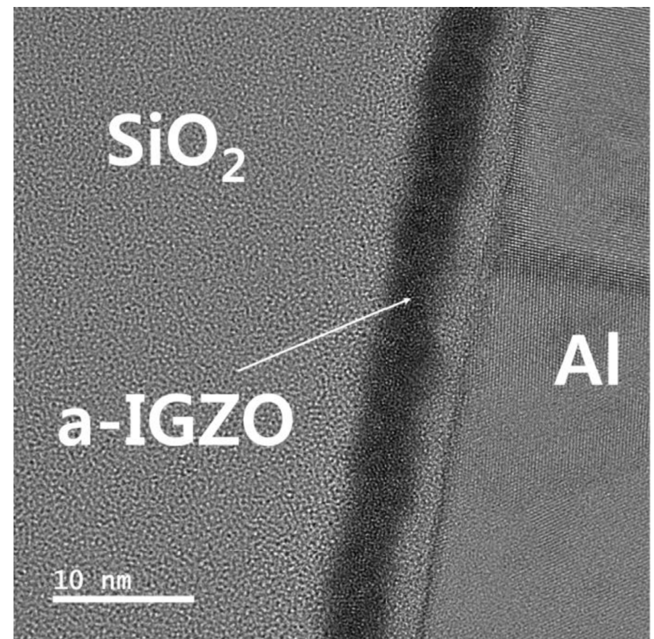

FIGURE 1. An HR-TEM cross-sectional image of a-IGZO TFT used in this study.

the contact characteristics in the S/D electrode regions are invariant for different humidity conditions. To measure the variations in the surface morphology and mechanical properties (hardness), AFM and AFM-nanoindentation were used. For the hardness measurements, a soft gold cantilever with a spring constant of 0.6 N/m was used. To study the variation in oxygen vacancies, the O_{1s} spectrum was measured using X-ray photoelectron spectroscopy (XPS).

III. RESULT & DISCUSSION

Figures 2 and 3 present evolutions of the transfer characteristics and extracted parameters of the a-IGZO TFTs, respectively, for dry and wet ambient conditions. Total five TFTs located in top, down, left, right, and center of a sample were measured in each graph in Fig. 2. The initial transfer curves (day 1) of the a-IGZO TFTs show good and uniform performance with average electrical parameters for a field effect mobility (μ_{FE}) of 4.20±0.15 cm^2/Vs, subthreshold slope (V_{SS}) of 0.92±0.18 V/dec, ON/OFF current ratio (I_{ON}/I_{OFF}) of 10^7 A/A, and threshold voltage (V_{TH}) of 6.30±0.27 V. The TFTs operated in enhancement mode.

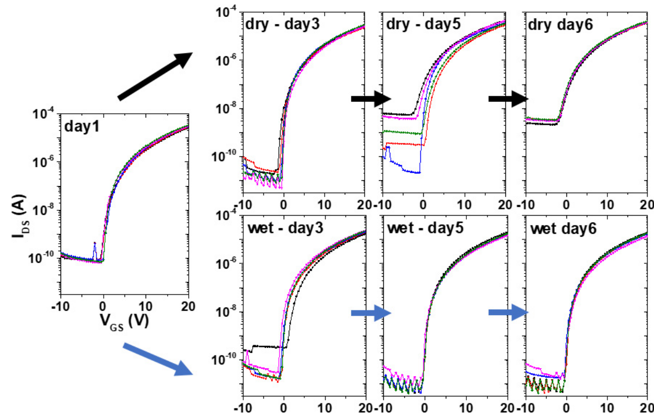

FIGURE 2. Transfer characteristics of a-IGZO TFTs on day 1, 3, 5, and 6 for different humidity conditions (V_{DS} = 80 V).

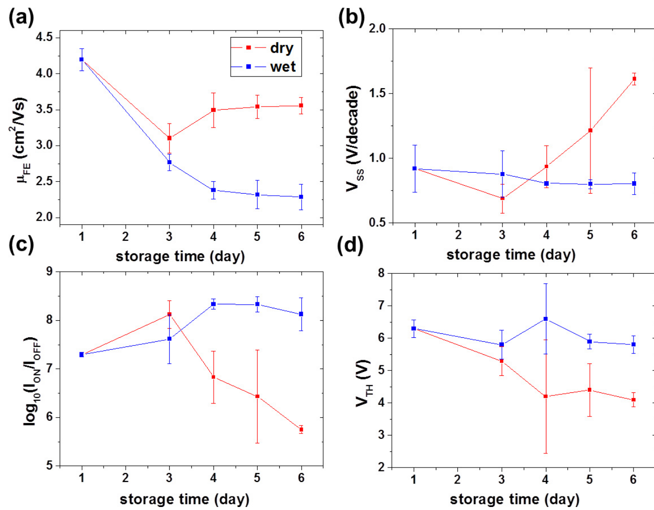

FIGURE 3. Storage time and humidity-dependent performance variations of a-IGZO TFTs. (a) Field-effect mobility in saturation regions (V_{DS} = 80 V), (b) subthreshold slope, (c) ON/OFF current ratio, and (d) threshold voltage.

After six days (day 6), the dry and wet samples exhibit significant differences in the transfer characteristics and electrical parameters. Both samples exhibit decreases in the field-effect mobility. However, the wet sample exhibits a greater decrease in the field-effect mobility, down to 2.28±0.18 cm^2/Vs, while that of the dry sample exhibits a relatively good performance of 3.56±0.11 cm^2/Vs even after six days shown in Fig. 3(a). Also, the V_{SS} values significantly increase from 0.92±0.18 to 1.61±0.05 V/decade for the dry samples, while it slightly decreases down to 0.80±0.08 V/decade for the wet samples shown in Fig. 3(b). At the same time, the I_{ON}/I_{OFF} values decrease to under 10^5 A/A for the dry samples, while they increase up to 10^8 A/A for the wet samples shown in Fig. 3(c). The threshold voltage (V_{TH}) shifts slightly in the negative direction for the dry sample, while it does not vary for the wet sample shown in Fig. 3(d). It is noted that, as the exposure time further increases, the off current level of the dry sample will continuously increase, while the on current level of the wet sample will continuously decrease. Eventually, the dry and wet samples will become different states, which are similar with open and short circuit faults, respectively.

The relationships between μ_{FE}, V_{SS}, V_{TH} and I_{ON}/I_{OFF} are closely related to the variations in donor- and acceptor-like states in the active layer [17], [18]. After a long period of exposure to dry ambient, oxygen vacancies are easily induced, which act as donor-like states in the active layer. Because the carrier density in the active region increases when oxygen vacancies are induced, the increase in V_{SS}, the negative shift of V_{TH} and the decrease in I_{ON}/I_{OFF} are well explained by the increase in oxygen vacancies and the carrier density for the dry sample. On the contrary, the wet sample exhibits different behavior. It has been known that water acts as donor-like states in the a-IGZO active layer for a small amount of exposure to water [14]. In this case, an assumption for the role of the water is that there is no chemical reaction between water and the a-IGZO active layer. In the low humidity condition, our work reproduces the prior results reported in the literature. However, after the active layer is exposed to high humidity for a long period, the water decreases the carrier density in the active layer, leading to a decrease in V_{SS} and increase in I_{ON}/I_{OFF}. This indicates that water induces acceptor-like states under long periods exposure. The origin of the generation of acceptor-like states is related to solubility of the a-IGZO active layer in water. There are prior results showing the a-IGZO active layer can be dissolved in the water. First, the water can be used as solvent to fabricate solution-processed a-IGZO TFTs [19]. In addition, the a-IGZO TFTs can be used as water-soluble devices [20]. Accordingly, the a-IGZO active layer can react with water even after annealing process is done, which follows chemical reactions given as [20],

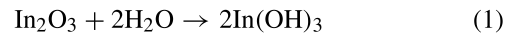

$$In_2O_3 + 2H_2O \rightarrow 2In(OH)_3 \quad (1)$$

$$ZnO + H_2O \rightarrow Zn(OH)_2 \quad (2)$$

$$2GaO(OH) + H_2O \rightarrow Ga_2O + 4(OH) \quad (3)$$

Further systematic study is required to understand the high humidity effect because the reaction time is different whether the active layer is exposed to humidity or dipped into water. It is understood that the generation of the acceptor-like states is originated from chemically induced defects of the a-IGZO active layer after exposure to water, which can be confirmed by the scanning electron microscopy (SEM) and AFM images.

Figures 4(a) and (b), and 4(c) and (d) present SEM and AFM images of the dry and wet samples after five days, respectively. There is a bright spot and spike-like shape region in the wet sample, which are due to the mechanical peeling of the active layer (Fig. 4(b)), while the dry sample shows a relatively clean surface (Fig. 4(a)). The peeling region also observed in an AFM image (Fig. 4(d)), which leads to a severe increase in surface roughness of the wet sample up to about 50 nm. On the contrary, the dry sample shows a small roughness under 2.0 nm in the AFM image

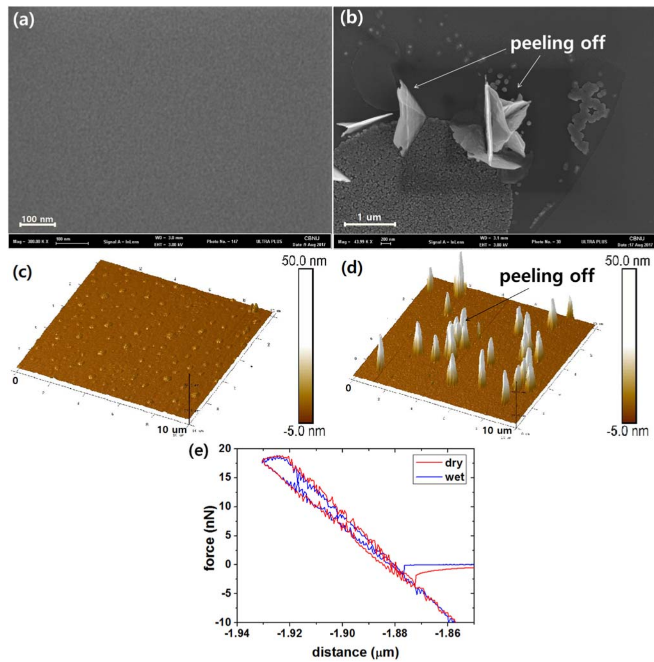

FIGURE 4. SEM images of (a) dry and (b) wet samples, and AFM images (10 × 10 μm) of (c) dry and (d) wet samples after five days. Surface peeling can be found in the wet sample. (e) AFM nanoindentation measurement results of dry and wet samples after five days.

(Fig. 4(c)). This indicates that the high-humidity condition severely decreases the film quality by lowering the mechanical adhesion properties and generates additional acceptor-like defect states in the bandgap region. It should be noted that the reaction between the a-IGZO active layer and the water is irreversible, which means the wet sample cannot be recovered. Unlike conventional environmental stress condition, the high humidity exposure condition critically influences on the a-IGZO TFT performance due to permanent surface damage shown in SEM and AFM images.

On the contrary, the hardness of the a-IGZO TFTs is invariant under the high-humidity conditions. Figure 4(e) presents the AFM nanoindentation measurement results of the dry and wet samples after five days. The force-to-distance ratio represents the relative hardness of the a-IGZO active layer. The resulting ratio is about 0.366 and 0.359 mN/m for the dry and wet samples during the loading processes, respectively. The variation in hardness is smaller than 2%. This indicates that the long-period high-humidity conditions do not severely degrade the hardness of the a-IGZO active layer. Instead, they induce mechanical peeling of the active layer in weakly bonded regions and generate many sub-micro-size defects in the active layer. It should be noted that the additional acceptor-like defect states are deep states because there is no variation in V_{SS} in the wet sample, as shown in Fig. 3(b). It is well-known that the heavy metal cation s-orbital is the main electron conduction path for the a-IGZO TFTs, which is strongly susceptible to disorder in the amorphous-based TFTs. For this reason, the subthreshold slope, which is related to the number of tail states, is relatively invariant to the creation of large defects in the active layer.

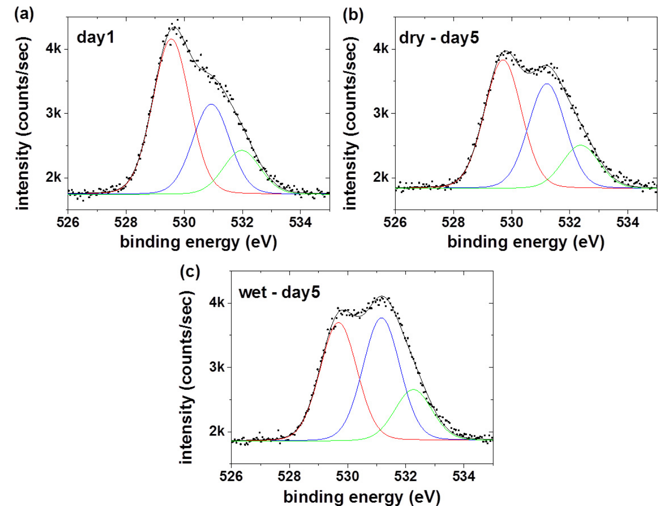

FIGURE 5. XPS measurements results of (a) day 1 and (b) day 5 of dry sample, and (c) day 5 of wet sample.

To verify the variations in oxygen-related defect state in the active layer, XPS measurements were performed for the dry and wet samples after five days. Unlike vacuum-processed a-IGZO TFTs which have relatively thick active layer (over 50 nm), the solution-processed a-IGZO TFTs have very thin active layer, typically under 10 nm [21], which is consistent with the TEM image in Fig. 1. The XPS signal can be obtained up to several nanometers under the surface of the active layer. Therefore, using the XPS data, composition of the channel region near the a-IGZO/SiO_x can be easily estimated. In addition, for the ambient stability experiments, variations of material properties in the bulk region are important because the bulk region is directly affected by the ambient. It critically influences on the electrical parameters of the TFTs such as μ_{FE}, V_{TH}, V_{SS}, and I_{ON}/I_{OFF} [22]. Therefore, using the XPS data in the bulk region, the variations of the electrical characteristics of the a-IGZO TFTs can be investigated.

Figures 5(a) to (c) presents the XPS spectra, including the deconvolution data, and Table 2 summarizes the relative area of the deconvolution graph. The peak binding energies of the deconvolution data are about 529.55 (low energy), 530.93 (middle energy), and 531.98 eV (high energy). Each peak is related to the oxygen in the lattice, vacancy, and -OH peak, respectively. The trend of the increase in oxygen vacancies and decrease in oxygen in the lattice is the same for the dry and wet sample after five days. The low-energy region decreases from 53.6 (reference) to 46.4 (dry sample) and 42.6 (wet sample), while the mid-energy region increases from 31.2 to 37.9 (dry sample) and 41.1 (wet sample). In this case, the high-energy peak does not vary, depending on the ambient conditions. It is noted that the increase in oxygen vacancies in the wet sample is higher than that in

TABLE 2. Relative area under the deconvoluted curves calculated from XPS data.

Devices \ Binding Energy		Low energy (%)	Middle energy (%)	High energy (%)
1st day		53.6	31.2	15.2
5th day	Dry	46.4	37.9	15.7
	Wet	42.6	41.1	16.3

TABLE 3. Parameters used in the technology-CAD simulation.

Devices \ Parameters	N_{GA} (cm^{-3} eV^{-1})	N_{GD} (cm^{-3} eV^{-1})	n (cm^{-3})	μ (cm^2 V^{-1} s^{-1})
Reference (1st day)	5.0×10^{16}	1.0×10^{21}	1.0×10^{17}	6.9
Dry	5.0×10^{16}	4.0×10^{21}	4.0×10^{17}	6.9
Wet	1.9×10^{17}	2.6×10^{20}	5.5×10^{17}	4.5

the dry sample. This is closely related to the amount of exposure area to ambient of the active layer. When the a-IGZO active layer reacts with water, the peeling regions are formed leading to an increase of a contact area to ambient in a-IGZO active layer. It is well known that an increase of exposure area to ambient accelerates an increase of the oxygen vacancies from the weak bonding sites of the lattice because dissociation of the oxygen atoms from the lattice are easily induced when the active layer is exposed to the ambient. Therefore, it is thought that the peeling region induces an increase of acceptor-like states (from dangling bond) and donor-like states (from oxygen vacancies), at the same time. From the XPS data, for the dry sample, it is understood that the negative shift of V_{TH}, decrease in I_{ON}/I_{OFF} and increase in V_{SS} originate from the increase in donor-like oxygen vacancies, leading to the increase in electron density in the active region. However, for the wet sample, there should be additional defect state generation to compensate for the increase in oxygen vacancies, implying that the generated electrons from the oxygen vacancies should be reduced to show the high I_{ON}/I_{OFF}, small shift of V_{TH} and low V_{SS}, as shown in Figs. 5(b) and (c).

Based on the discussion, there are three important mechanisms to degrade the electrical performance of solution-processed a-IGZO TFTs exposed to a high humidity for a long period; the increase in electron density from the generation of oxygen vacancies, the increase in deep acceptor-like states, and the decrease in the Hall mobility originating from the peeling region. This can be confirmed by simulation fitting using an ATLAS 2D device simulator (from Silvaco Inc.). For the simulation fitting, we selected a-IGZO TFTs of which the electrical parameters are close to the average values in Figs. 3(a) to (d). In particular, day 1 (reference) and day 6 (dry and wet) samples were selected for the simulation fitting because they are initial and final storage conditions. It should be noted that the TFTs of day 1 and day 6 show very small standard deviations as shown in Figs. 3(a) to (d). Accordingly, the accuracy of the simulation fitting can be guaranteed.

Only bulk region defect DOS variations were considered, because the bulk region is directly affected by the water in ambient and the a-IGZO TFTs are mainly dependent on the chemical and mechanical variations of the bulk region. For ON current region, we considered acceptor-like states in the upper bandgap region. First, the reference data (day 1) were fitted to the simulation result. The obtained parameters were as follows: maximum conduction band tail states (N_{TA}) = 6.0×10^{19} cm^{-3} eV^{-1}, width of conduction band tail states (W_{TA}) = 65 meV, conduction band deep states (N_{GA}) = 5.0×10^{16} cm^{-3} eV^{-1}, electron density (n) = 1.0×10^{17} cm^{-3}, and Hall mobility (μ) = 6.9 cm^2 V^{-1} s^{-1}. The conduction band deep states were assumed to be flat with a large width (W_{GA} = bandgap). For the dry sample, using the reference parameters, the transfer characteristics were fitted by varying only one parameter; electron density. For the wet sample, the electron density of the sample was calculated from the XPS data and fitting data of the reference and dry samples assuming partial ionization of the oxygen vacancies. The ratio of the ionized oxygen vacancies was calculated by 31.2 – x (reference):37.9 – x (dry sample) = 1.0×10^{17}: 4.0×10^{17}, where x is the portion of unionized oxygen vacancies. The x was about 29.0% and the electron density of the wet sample can be calculated by $(41.1 – x) \times 10^{17} = 5.5 \times 10^{17}$. Then, by varying two parameters of N_{GA} and μ, the simulation result was fitted to the experimental result. The fitted N_{GA} and μ were 1.9×10^{17} cm^{-3} eV^{-1} and 4.5 cm^2 V^{-1} s^{-1}, respectively.

For OFF current region, we considered valence band deep states because the off current level depends on electron density and valence band deep states [17]. After initial fitting of the reference parameters, all the parameters of the dry and wet sample of the valence band deep states were determined from the N_{GA} and n. The variations of valence band deep states were simulated by varying N_{GD} (maximum valence band deep states) with constant W_{GD} = 0.10 eV (width of valence band deep states) [17]. Because the dry sample shows an increase of oxygen vacancies and the origin of valence band deep states is oxygen vacancies, N_{GD} of the dry sample increases compared to the reference. Accordingly, the N_{GD} value was determined by increasing N_{GD} value for the dry sample. On the contrary, for the wet sample, because of a negative-U characteristic which shows a reverse relationship between N_{GA} and N_{GD}, valence band deep states decreases though the electron density increases [22]. Accordingly, the N_{GD} value was determined by decreasing N_{GD} for the wet sample. All the fitting parameters are summarized in Table 3.

Figure 6 shows the transfer characteristics of the simulation results when V_{GS} varies from 0 to 40 V and

JOURNAL OF THE
ELECTRON DEVICES SOCIETY

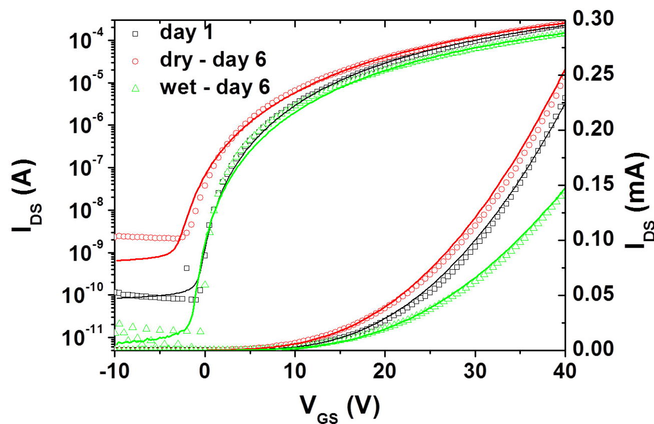

FIGURE 6. **Simulation and experimental results of transfer characteristics of a-IGZO TFTs using technology-CAD simulator (scatter: experiments, line: simulation).**

$V_{DS} = 80$ V. It can be seen that all the simulation results fit well with the experimental results. It should be noted that the acceptor-like deep states of the wet sample are about four times larger than those of the reference without varying the tail states, which is consistent with the V_{SS} data. This clearly indicates that the H_2O induces mechanical degradation and induces acceptor-like states in the a-IGZO active layer under long-period exposure. This compensates the increase in electron density coming from the oxygen vacancies, which is consistent with the SEM and AFM data.

IV. CONCLUSION

In conclusion, the effect of long-period high-humidity exposure on solution-processed a-IGZO TFTs was investigated. It is demonstrated that mechanical peeling of the active layer is induced under high-humidity conditions, leading to acceptor-like deep states and compensation for the increase in electron density coming from the oxygen vacancies in the active layer. Unlike the conventional role of water in the a-IGZO active layer, the high-humidity conditions induce additional effects, including a decrease in the adhesion properties, which results in a severe decrease in the performance of the solution-processed a-IGZO TFTs. Performance degradation can also be observed in other solution-processed oxide-based TFTs. Therefore, improvements in the adhesion properties of a-IGZO TFTs are essential to increase the lifetime of solution-based TFTs.

REFERENCES

[1] T. Kamiya, K. Nomura, and H. Hosono, "Present status of amorphous In–Ga–Zn–O thin-film transistors," *Adv. Mater.*, vol. 11, no. 4, pp. 044305–044328, 2010.

[2] M. Niko, K. H. Cherenack, and G. Troster, "The effects of mechanical bending and illumination on the performance of flexible IGZO TFTs," *IEEE Trans. Electron Devices*, vol. 58, no. 7, pp. 2041–2048, Jul. 2011.

[3] D.-H. Lee, S.-Y. Han, G. S. Herman, and C.-H. Chang, "Inkjet printed high-mobility indium zinc tin oxide thin film transistors," *J. Mater. Chem.*, vol. 19, no. 20, pp. 3135–3137, 2009.

[4] S. K. Park, Y.-H. Kim, and J.-I. Han, "All solution-processed high-resolution bottom-contact transparent metal-oxide thin film transistors," *J. Phys. D Appl. Phys.*, vol. 42, no. 12, pp. 125102–125105, 2009.

[5] C.-S. Fuh, P.-T. Liu, Y.-T. Chou, L.-F. Teng, and S. M. Sze, "Role of oxygen in amorphous In–Ga–Zn–O thin film transistor for ambient stability," *ECS J. Solid-State Sci. Technol.*, vol. 2, no. 1, pp. Q1–Q5, 2013.

[6] H. S. Shin, Y. S. Rim, Y.-G. Mo, C. G. Choi, and H. J. Kim, "Effects of high-pressure H_2O-annealing on amorphous IGZO thin-film transistors," *Physica Status Solidi (A)*, vol. 208, no. 9, pp. 2231–2234, 2011.

[7] P. N. Plassmeyer, G. Mitchson, K. N. Woods, D C. Johnson, and C. J. Page, "Impact of relative humidity during spin-deposition of metal oxide thin films from aqueous solution precursors," *Chem. Mater.*, vol. 29, no. 7, pp. 2921–2926, 2017.

[8] S. Sung *et al.*, "Effects of ambient atmosphere on the transfer characteristics and gate-bias stress stability of amorphous indium-gallium-zinc oxide thin-film transistors," *Appl. Phys. Lett.*, vol. 96, no. 10, 2010, Art. no. 102107.

[9] S. Lee and J. Jeong, "Inert gas annealing effect in solution-processed amorphous indium-gallium-zinc-oxide thin-film transistors," *J. Korean Phys. Soc*, vol. 71, no. 4, pp. 209–214, 2017.

[10] W.-T. Chen *et al.*, "Oxygen-dependent instability and annealing/passivation effects in amorphous In–Ga–Zn–O thin-film transistors," *IEEE Electron Device Lett.*, vol. 32, no. 11, pp. 1552–1554, Nov. 2011.

[11] D. Kim *et al.*, "Role of adsorbed H_2O on transfer characteristics of solution-processed zinc tin oxide thin-film transistors," *Appl. Phys. Exp.*, vol. 5, no. 2, pp. 21101–21109, 2012.

[12] W.-F. Chung *et al.*, "Influence of H_2O dipole on subthreshold swing of amorphous indium-gallium-zinc-oxide thin film transistors," *Electrochem. Solid-State Lett.*, vol. 14, no. 3, pp. H114–H116, 2011.

[13] S. J. Kim, S. Yoon, and H. J. Kim, "Review of solution-processed oxide thin-film transistors," *Jpn. J. Appl. Phys.*, vol. 53, no. 2S, 2014, Art. no. 02BA02.

[14] M. D. H. Chowdhury *et al.*, "Effect of SiO_2 and SiO_2/SiN_x passivation on the stability of amorphous indium-gallium zinc-oxide thin-film transistors under high humidity," *IEEE Trans. Electron Devices*, vol. 62, no. 3, pp. 869–874, Mar. 2015.

[15] G. H. Kim *et al.*, "Effect of indium composition ratio on solution-processed nanocrystalline InGaZnO thin film transistors," *Appl. Phys. Lett.*, vol. 94, no. 23, 2009, Art. no. 233501.

[16] B. S. Jeong, Y. G. Ha, J. Moon, A. Facchetti, and T. J. Marks, "Role of gallium doping in dramatically lowering amorphous-oxide processing temperatures for solution-derived indium zinc oxide thin-film transistors," *Adv. Mater.*, vol. 22, no. 12, pp. 1346–1350, 2010.

[17] J. Jeong and Y. Hong, "Debye length and active layer thickness-dependent performance variations of amorphous oxide-based TFTs," *IEEE Trans. Electron Devices*, vol. 59, no. 3, pp. 710–714, Mar. 2012.

[18] T. Fung *et al.*, "Two-dimensional numerical simulation of radio frequency sputter amorphous In–Ga–Zn–O thin-film transistors," *J. Appl. Phys*, vol. 106, no. 8, 2009, Art. no. 084511.

[19] G. Liu *et al.*, "Low-temperature, nontoxic water-induced metal-oxide thin films and their application in thin-film transistors," *Adv. Funct. Mater.*, vol. 25, no. 17, pp. 2564–2572, 2015.

[20] S. H. Jin *et al.*, "Water-soluble thin film transistors and circuits based on amorphous indium-gallium-zinc-oxide," *ACS Appl. Mater. Interfaces*, vol. 7, no. 15, pp. 8268–8274, 2015.

[21] Y.-H. Kim *et al.*, "Flexible metal-oxide devices made by room-temperature photochemical activation of sol-gel films," *Nature*, vol. 489, pp. 128–133, Sep. 2012.

[22] K. Ide *et al.*, "Effects of excess oxygen on operation characteristics of amorphous In-Ga-Zn-O thin-film transistors," *Appl. Phys. Lett.*, vol. 99, no. 9, pp. 1–3, 2011.

SEUNG-UN LEE received the M.S. degree in information and communication from Chungbuk National University, Chungju, South Korea, in 2018. He is currently a Researcher with the Ulsan National Institute of Science and Technology, Ulsan, South Korea. His current research interests include design and fabrication of photo detector with hybrid halide perovskite for sensor applications.

JAEWOOK JEONG received the B.S. and M.S. degrees in physics and the Ph.D. degree in electrical engineering from Seoul National University, Seoul, South Korea, in 2003, 2005, and 2010, respectively. Since 2015, he has been with the School of Information and Communication Engineering, Chungbuk National University, Cheongju, South Korea, where he is currently an Associate Professor.